Advances in Science and Technology Research Journal

Advances in Science and Technology Research Journal 2022, 16(4), 119–129
https://doi.org/10.12913/22998624/152172
ISSN 2299-8624, License CC-BY 4.0

Received: 2022.06.19
Accepted: 2022.08.22
Published: 2022.09.01

Tooth Contact Analysis of Cylindrical Gears with an Unconventional Tooth Profile

Michał Batsch[1*], Dawid Wydrzyński[1], Łukasz Przeszłowski[1]

[1] Faculty of Mechanical Engineering and Aeronautics, Department of Mechanical Engineering, Rzeszow University of Technology, al. Powstańców Warszawy 8, 35-959 Rzeszów, Poland

* Corresponding author's e-mail: mbatsch@prz.edu.pl

ABSTRACT

The paper presents mathematical models of cylindrical gear pairs with various types of tooth profiles, such as eccentric-cycloidal, concavo-convex Novikov type, and involute. Comparative analyses were provided for the aforementioned gear meshes, aimed at determining contact patterns, sliding velocity, and transmission errors. Tooth surface modifications were also considered. The results were compared with findings for a conventional involute gearing. It was found that the contact pattern in Novikov conformal gearing is 30% greater than in the involute gear pair, and 60% greater than in the eccentric-cycloidal gear pair. The smallest sliding velocity was obtained in Novikov gearing, which may be beneficial in terms of durability.

Keywords: eccentric-cycloidal gearing, involute gearing, Novikov gearing, contact pattern, sliding velocity, transmission error.

INTRODUCTION

Cylindrical gear pairs are commonly applied in nearly all branches of industry. Growing requirements placed on gear pairs, such as increased load-carrying capacity, improved noise behaviour, low weight or reliability, have prompted researchers and engineers to look for increasingly novel technological and design solutions. More and more attention is drawn to new manufacturing technologies like DMLS [1], as well as new tooth finishing techniques [2]. Novel types of calculation procedures aiming at gear mass reduction [3] as well as more accurate surface strength and wear prediction [4] are also within the interests of gear scientists and engineers. In addition, designers look for new tooth profiles which could provide an alternative to the commonly used involute profile. A recently published review paper [5] extensively discusses the literature concerning the non-involute external gears. The authors compared various types of gear meshes in terms of surface durability, root load capacity, gear efficiency, vibration, and sensitivity to assembly and manufacturing errors. Fourteen types of gear profiles were compared such as: cycloid gears [6], Novikov gears [7], triple circular-arc gears [8], cosine gears [9], double circular arc involute gears [10], S-gears [11], and pure rolling helical gears [12]. From all referenced above types of tooth profiles, the greatest surface durability and the smallest heat load are assigned to pure rolling transmission, S-gears, and conformal gearings (Novikov gears or W-N gears). Pure rolling transmission operation is similar to Novikov gears. The continuity of meshing is realized by overlap. The tooth profiles may be chosen arbitrarily however the contact point should lay on point of tangency of pitch circles to avoid sliding velocity. In paper [13] authors proposed the tooth profiles of pure rolling transmission formed by circular arcs with the convexo-convex type of contact. They have investigated proposed gearing in terms of contact stresses and loaded transmission error

[13]. The pure rolling type of transmission was also investigated in gear-rack [14] and internal helical [15] gear mesh. S-gears are gears, which profile is formed by a rack with an analytically defined profile by power function [16]. The transverse line of action of this type of gearing is curvilinear and therefore may offer a greater contact ratio than conformal or pure rolling gearing. The advantage of this kind of gear mesh is reduced sliding velocity in comparison with the involute one which was reported in [17]. This type of gear profile was proposed for polymer gears [18]. Novikov gears also offer reduced sliding in comparison with involute gears and due to conformal contact may be beneficial in terms of surface strength. Successful application of Novikov gears [19] prompts the scientist to continue the research on this kind of gearing [7,20]. Another non-conventional tooth profile is the so-called eccentric-cycloidal tooth profile. This kind of gearing is a special case of helical cycloid gear drive where the pinion tooth profile is formed by the circular arc and the conjugated gear wheel profile is an internal equidistant of the epicycloid [21]. The-above referenced gear teeth profile is not well researched and described in the literature. Therefore, the aim of this paper is to compare three types of cylindrical gear pairs: an involute gear pair, a Novikov gear pair [7,20], and an eccentric-cycloidal gear pair [21,22].

MATHEMATICAL MODEL OF CYLINDRICAL GEAR MESH

The analysis will concern cylindrical reduction gear pairs with parallel axes and external meshing. Moving coordinate systems 1 and 2 connected, respectively, with the drive gear (the pinion) and the driven gear (the gear wheel) were set up. The gears rotate around axes z_1 and z_2 by angles φ_1 and φ_2 in in the indicated directions of angular velocities ω_1 and ω_2 (Figure 1). Tooth surfaces are represented in appropriate coordinate systems $\bar{r}_1^{(1)}(\theta_1, \zeta_1)$ and $\bar{r}_2^{(2)}(\theta_2, \zeta_2)$.

Moreover, fixed coordinate system *f* connected with the transmission body was introduced, wherein axis z_f corresponds to axis z_1 of the pinion's coordinate system. The gear wheel's rolling cylinders with diameters d_{t1} and d_{t2} are separated by centre distance a_r. In order to take into account axis position deviations due to assembly or workmanship errors, or elastic deformations of shafts and bearings, the coordinate system connected with the gear wheel must be shifted along axis x_f, y_f, z_f by Δa_x, Δa_y and Δa_z, and then rotated relative to fixed axes parallel to axes x_f and y_f, respectively, by angles κ_x and κ_y. For this purpose, additional coordinate system *h* was introduced (Figure 2).

Allowing for errors, the gear will rotate around the new shifted and skewed axis z_h=z_2. In the context of Figures 1 and 2, transformation matrices from system *f* are given as (1) and (2):

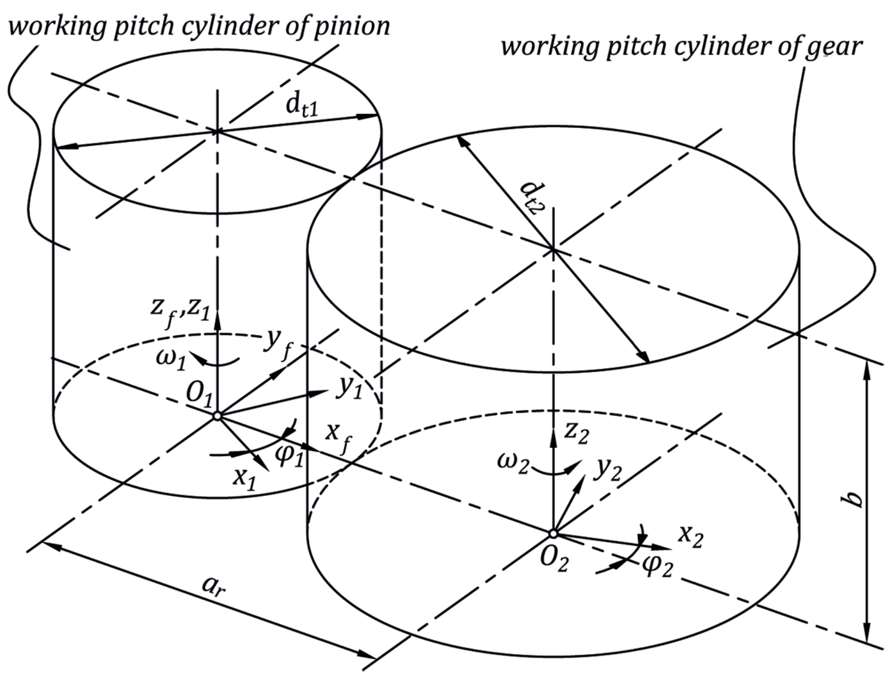

Figure 1. Coordinate systems set up in the cylindrical gear pair mesh analysis

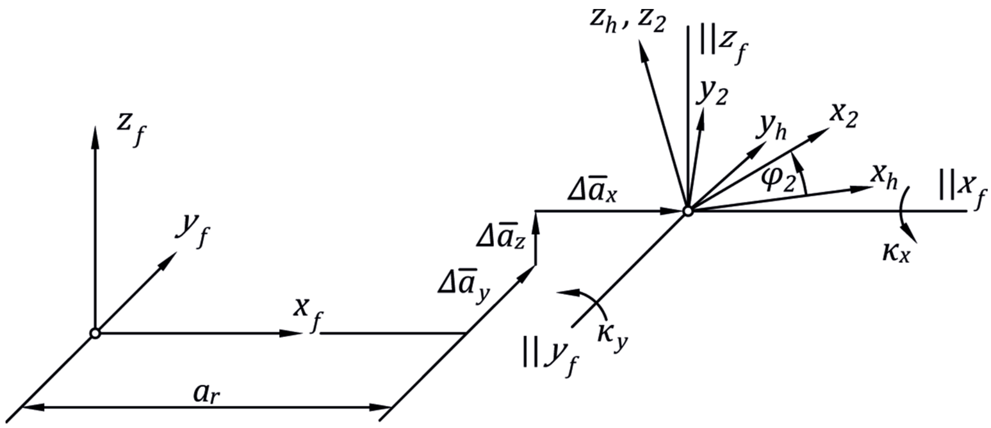

Figure 2. The position and orientation of additional coordinate system h

$$M_{f1} = \mathrm{Rot}(-\varphi_1, Z) \tag{1}$$

$$M_{f2} = M_{fh} M_{h2} \tag{2}$$

where: matrices M_{h2} and M_{fh} are given as (3) and (4):

$$M_{h2} = \mathrm{Rot}(\varphi_2, Z) \tag{3}$$

$$\begin{gathered} M_{fh} = \mathrm{Rot}(\kappa_y, Y) \cdot \mathrm{Rot}(\kappa_x, X) \cdot \\ \cdot \mathrm{Tr}(a_r + \Delta a_x, X) \cdot \mathrm{Tr}(\Delta a_y, Y) \cdot \mathrm{Tr}(\Delta a_z, Z) \end{gathered} \tag{4}$$

Then, tooth surfaces in the fixed coordinate system can be expressed as (5) and (6):

$$\bar{r}_1^{(f)} = \begin{bmatrix} x_1^{(f)} \\ y_1^{(f)} \\ z_1^{(f)} \\ 1 \end{bmatrix} = M_{f1} \bar{r}_1^{(1)} \tag{5}$$

$$\bar{r}_2^{(f)} = \begin{bmatrix} x_2^{(f)} \\ y_2^{(f)} \\ z_2^{(f)} \\ 1 \end{bmatrix} = M_{f2} \bar{r}_2^{(2)} \tag{6}$$

This study discusses three types of gear pairs with helical teeth, wherein the pinion has a right-hand and the gear has a left-hand flank pitch line:

(a) The involute gear pair

$$\bar{r}_1^{(1)} = \begin{bmatrix} r_{b1}(\cos(\zeta_1 + t_1 - \varphi_{sym1}) + t_1 \sin(\zeta + t_1 - \varphi_{sym1})) \\ r_{b1}(\sin(\zeta_1 + t_1 - \varphi_{sym1}) - t_1 \cos(\zeta_1 + t_1 - \varphi_{sym1})) \\ r_1 \zeta_1 \mathrm{ctg}\beta \\ 1 \end{bmatrix} \tag{7}$$

$$\bar{r}_2^{(2)} = \begin{bmatrix} r_{b2}(-\cos(\zeta_2 - t_2 + \varphi_{sym2}) + t_2 \sin(\zeta - t_2 + \varphi_{sym2})) \\ r_{b2}(\sin(\zeta_2 + t_2 + \varphi_{sym2}) + t_2 \cos(\zeta - t_2 + \varphi_{sym2})) \\ r_2 \zeta_2 \mathrm{ctg}\beta \\ 1 \end{bmatrix} \tag{8}$$

where: r_{b1}, r_{b2} are base radii of, respectively, the pinion and the gear,
t_1, t_2 are gear and pinion tooth profile parameters (rolling angles),
ζ_1, ζ_2 are the parameters of the helical line of the pinion and the gear,
β is the inclination angle of the flank pitch line on the pitch cylinder,
r_1 and r_2 are the pitch radii of, respectively, the pinion and the gear [23].

(b) The Novikov gear pair

$$\bar{r}_1^{(1)} = \begin{bmatrix} \rho_1 \cos(\theta_1 + \zeta_1) + r_1 \cos\zeta_1 - d_{CO'} \sin(\alpha_t + \zeta_1) \\ \rho_1 \sin(\theta_1 + \zeta_1) + r_1 \sin\zeta_1 + d_{CO'} \cos(\alpha_t + \zeta_1) \\ r_1 \zeta_1 \mathrm{ctg}\beta \\ 1 \end{bmatrix} \tag{9}$$

$$\bar{r}_2^{(2)} = \begin{bmatrix} \rho_2 \cos(\theta_2 + \zeta_2) - r_2 \cos\zeta_2 - (\rho_2 - \rho_1 + d_{CO'}) \sin(\alpha_t - \zeta_2) \\ \rho_2 \sin(\theta_2 + \zeta_2) + r_2 \sin\zeta_2 + (\rho_2 - \rho_1 + d_{CO'}) \cos(\alpha_t - \zeta_2) \\ r_2 \zeta_2 \mathrm{ctg}\beta \\ 1 \end{bmatrix} \tag{10}$$

where: θ_1, θ_2 are profile parameters,
ζ_1, ζ_2 are helix parameters for the pinion and the gear, respectively,
α_t is the face pressure angle,
ρ_1 is the convex tooth profile radius,
ρ_2 is the concave tooth profile radius,
while r_1 and r_2 are pitch circle radii [7].

(c) The eccentric-cycloidal gear pair

$$\bar{r}_1^{(1)} = \begin{bmatrix} g\cos(\eta_1 + \zeta_1) + e\cos\zeta_1 \\ g\sin(\eta_1 + \zeta_1) + e\sin\zeta_1 \\ r_1 \zeta_1 \mathrm{ctg}\beta \\ 1 \end{bmatrix} \tag{11}$$

$$\bar{r}_2^{(2)} = \mathrm{Rot}(\pi - \zeta, Z) \cdot \mathrm{Tr}(r_2\zeta_2 \mathrm{ctg}\beta, Z) \cdot$$
$$\cdot \begin{bmatrix} r_1\left((i_{12}+1)\cos\eta_2 - \lambda\cos((i_{12}+1)\eta_2) + \nu\dfrac{\cos\eta_2 - \lambda\cos((i_{12}+1)\eta_2)}{\sqrt{1-2\lambda\cos(i_{12}\eta_2)+\lambda^2}}\right) \\ r_1\left((i_{12}+1)\sin\eta_2 - \lambda\sin((i_{12}+1)\eta_2) + \nu\dfrac{\sin\eta_2 - \lambda\sin((i_{12}+1)\eta_2)}{\sqrt{1-2\lambda\cos(i_{12}\eta_2)+\lambda^2}}\right) \\ 0 \\ 1 \end{bmatrix} \quad (12)$$

where: η_1 – the profile parameter,
ζ_1 – the parameter of the pinion flank line,
$g = \nu r_1$ – the pinion tooth profile radius,
ν – the equidistant shift ratio (for an internal equidistant, $\nu < 0$), and
λ – the tooth height ratio,
e – the eccentric,
r_1 and r_2 – pitch circle radii [22].

TOOTH FLANK SURFACE MODIFICATION

Tooth flank surface modification is a procedure wherein the tooth flank is deliberately tilted away from the nominal surface. Its purpose is to compensate for tooth workmanship errors, as well as gear position errors in the transmission box arising from elastic deformations of shafts, or bearing clearances (slackness). Standard [24] distinguishes between various types of modification, the basic of which include: tooth profile modification, tooth flank line modification, and topology modification. Tooth profile modification C_α (Figure 3a)) is generally implemented in order to reduce uneven load along the pressure segment. Tooth flank line modification C_β (Figure 3b)) can compensate for shaft deflections. The application of both modifications C_α+C_β (Figure 3c)) makes it possible to avoid edge contact, a phenomenon which may lead to stress concentration. In principle, any modification may be considered as an appropriately defined topological modification (Figure 3d)). Usually, however, topological modification C_Σ is understood as free-form modification – i.e. freely defined on the tooth surface grid.

The modification is conveniently defined and presented on coordinate grid $z_i = z_i^{(i)}$,

$$r_{yi} = \sqrt{(x_i^{(i)})^2 + (y_i^{(i)})^2}$$

where: index $i=1,2$ refers to the tooth surface of, respectively, the pinion and the gear.

If surface parameters are assigned to the profile and the tooth flank line, it may also be defined on their grid θ_i, ζ_i. If the modification was not included when generating the surface, e.g. by shaping the honing tool or its additional motions, it may be implemented with the use of relationship (13)

$$\bar{r}_i^{*(i)} = \bar{r}_i^{(i)} - C_i \bar{n}_i^{(i)} \quad (13)$$

where: $\bar{r}_i^{*(i)}$ – the vector of the modified surface,
$\bar{r}_i^{(i)}$ – the vector of a non-modified surface,

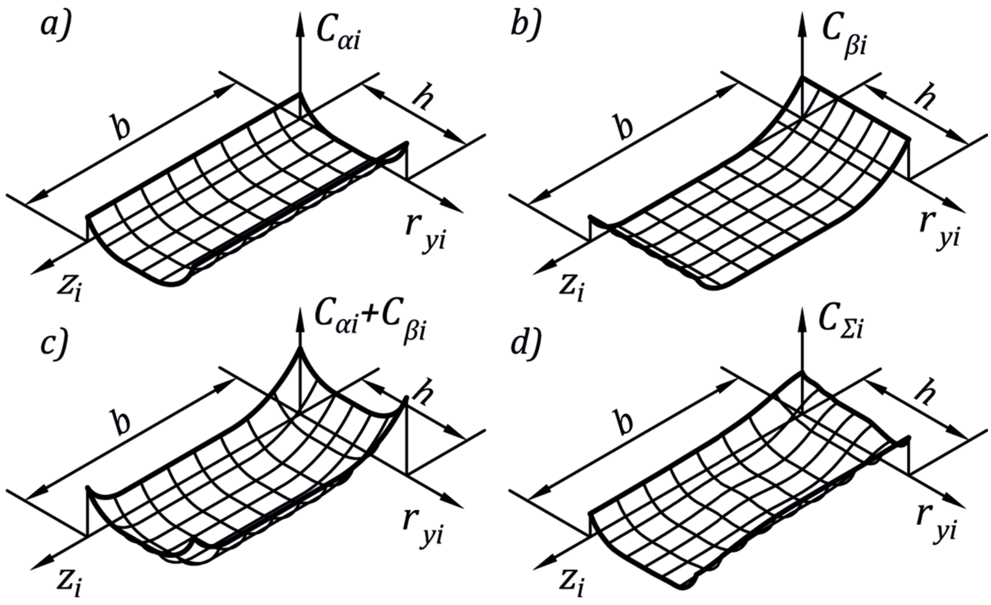

Figure 3. Types of tooth flank modifications: a) profile modification, b) flank line modification, c) simultaneous profile and flank line modification, d) topological modification, where b is the toothed ring width, and h is the tooth height

$\bar{n}_i^{(i)}$ – the versor normal to the non-modified surface,

C_i – the amount of modification.

In such a situation, instead of the non-modified surface, the analyses make use of the surface with a modification described by vector (13). Note that a positive modification is the modification deep into the material (towards the tooth) whereas the negative one is a modification to the outside of the material (towards the tooth space).

TRANSMISSION ERROR AND EASE-OFF TOPOGRAPHY

A method whereby surfaces can be given as discrete was used in order to determine transmission error and *Ease-Off* topography. Its concept was presented in [25]. The method was designed to analyse bevel and hypoid gear pairs, and implemented in *KIMoS*, a computer-aided bevel and hypoid gear pair design system by *Klingelnberg*. This section discusses the authors' implementation of the method.

It assumes a perfect mesh between pinion tooth Σ_1 and gear tooth surface Σ_2, i.e. one in which the gears are rotated by angles resulting from theoretical gear ratio $i_{12} = z_2/z_1 = \varphi_1/\varphi_2$. Surfaces in the n^{th} position are shown in Figure 4.

It is assumed that pinion rotation axis z_1 is aligned with axis z_f of fixed coordinate system f, and the surfaces in that system are given by vectors (3.1) and (3.2). In each position n resulting from the discretization of gear rotation angles, between the surfaces there is a certain distance measured along the arc with radius $R_{M2c}^{(f)} = \sqrt{\left(x_1^{(f)}\right)^2 + \left(y_1^{(f)}\right)^2}$ corresponding to the length of arc $k_{kor} = \widehat{M_1M_2}$, where M_1 is a point on surface Σ_1 with coordinates $z_1^{(f)}$, and M_2 a point on surface Σ_2 with coordinates $z_1^{(f)} = z_{M2c}^{(f)}$. Angle φ_{kor}, by which surface Σ_1 would have to be rotated in order for points M_1 and M_2 to overlap, is the central angle corresponding to the length of arc $k_{kor} = \widehat{M_1M_2}$ and can be determined on the basis of coordinates as (14):

$$\varphi_{kor} = \\ = 2\arcsin\left(\frac{\sqrt{\left(x_1^{(f)} - x_{M2c}^{(f)}\right)^2 + \left(y_1^{(f)} - y_{M2c}^{(f)}\right)^2}}{2R_{M2c}^{(f)}}\right) \tag{14}$$

The distance between flank surfaces is expressed as (15)

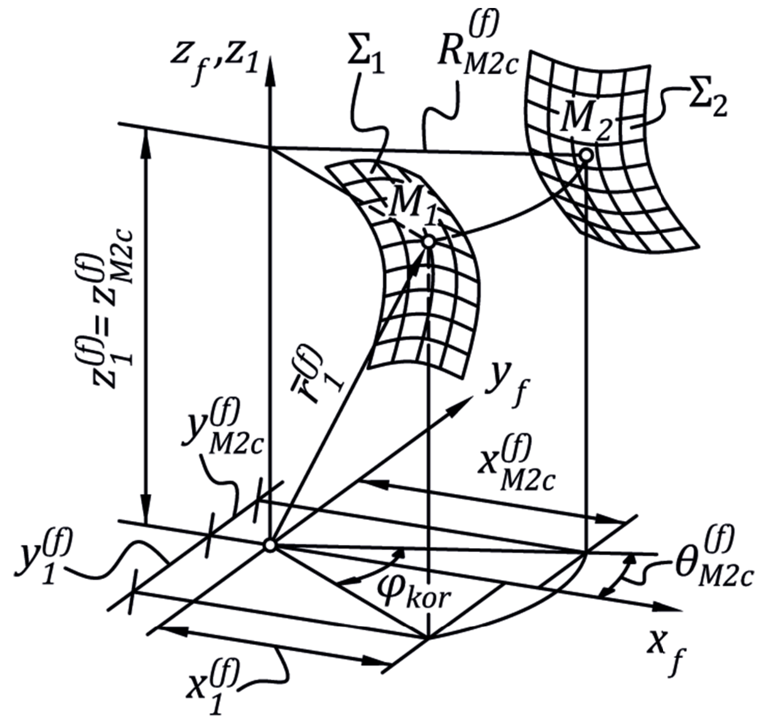

Figure 4. Tooth flanks in the n^th^ position

$$k_{kor} = R_{M2c}^{(f)} \varphi_{kor} \tag{15}$$

In each n^{th} position there is a certain minimum distance k_{kor}^{min} with its corresponding angle φ_{kor}^{min}. The relationship between minimum angle φ_{kor}^{min} and gear rotation angle φ_2 determined discretely for all n positions constitutes the transmission error. In addition, in a specific n^{th} position the distribution of distances k_{kor} on surface Σ_1 is referred to as an instantaneous *Ease-Off*. The *Ease-Off* is generated in the form of the lowest-lying envelope of instantaneous *Ease-Offs* for all n positions. The greatest challenge posed by the method is to specify the location of point M_2 on surface Σ_2 which corresponds to coordinate $z_1^{(f)} = z_{M2c}^{(f)}$ and radius $R_{M2c}^{(f)}$. The issue may be easily solved by interpolation in cylindrical coordinate system $\theta_{2c}^{(f)}, R_{2c}^{(f)}, z_2^{(f)}$.

GEOMETRIC CONTACT PATTERN

In a gear pair, the contact pattern is the area where contact takes place between mating tooth surfaces. It is created by the elastic deformation of teeth due to forces exerted in the meshing. A *geometric contact pattern* is defined as an approximation of the actual contact area based exclusively on the geometric properties of surfaces in contact. In other words, it is determined without taking into account the relationship between the deformation and forces applied or the type of material used.

There are many methods of determining the geometric contact pattern. They include, among others, methods based on mathematical models [26–28] and methods employing CAD systems [29,30]. The use of CAD systems involves the mutual penetration of three-dimensional tooth models to the depth corresponding to the thickness of the gear marking compound applied in gear pair tests, or the expected deformations. The contact pattern has the form of a flaky construct generated through the logical multiplication of thus positioned solid shapes. To visualise the movement of the contact pattern, the above operation must be performed for consecutive discrete positions arising from the rotation angles of gear solids. This approach was detailed in [31]. Its equivalent is the method which involves finding the curve of the intersection of tooth surfaces supplied in an analytical way [27]. Another method is the one proposed in [26]. The contact pattern is defined as the area for which the distance between the points on the surfaces in contact, measured along the common normal, is lower than the set amount. In order to determine the contact pattern, the method uses an approach similar to determining Hertz contact stress for point contact [32,33]. It is based only on the main curvatures of the surfaces, and the contact pattern resulting from the local approximation of surfaces is always elliptical [34]. The main drawback of this approach is that it is constrained to only local analysis, without taking into account e.g. edge contact. Moreover, it is of limited use for non-elliptical contact patterns which occur e.g. in gears with an eccentric-cycloidal profile [22] or Novikov gears with a concavo-convex profile [35]. The last method, described in more detail in this paper, is one in which contact pattern is determined as a set of points for which the distance between tooth flank surfaces, measured along unit normal to the pinion tooth flank, is lower than the set value [28]. The method makes it possible to determine edge and non-elliptical patterns, as verified experimentally for cylindrical Novikov gears [7] and eccentric-cycloidal meshing [22].

Let us consider a gear for which mating tooth surfaces Σ_1 and Σ_2 are given in a fixed coordinate system f by vectors (5) and (6). The contact pattern is determined on the basis of vector equation (16) resulting directly from Figure 5.

$$\bar{r}_1^{(f)}(\theta_1, \zeta_1) + k\bar{n}_1^{(f)}(\theta_1, \zeta_1) = \bar{r}_2^{(f)}(\theta_2, \zeta_2) \tag{16}$$

where: k – the distance between tooth flanks measured along unit normal to the pinion tooth surface. The above equation can be solved on the basis of distance k and gear tooth surface parameters θ_2, ζ_2 for all discrete pinion tooth surface parameters θ_1, ζ_1. The points for which distance k is smaller than the assumed value form the contact pattern. Assuming that gears revolve around axis z, the contact pattern is conveniently presented as a projection on plane r_{y1}, z_f, where $r_{y1} = \sqrt{(x_1^{(f)})^2 + (y_1^{(f)})^2}$ is an arbitrary radius of the pinion.

Solving vector equation (16) representing a system of three algebraic, usually non-linear equations, is problematic and time-consuming even if numerical methods are employed [36,37]. For this reason, it is recommended that

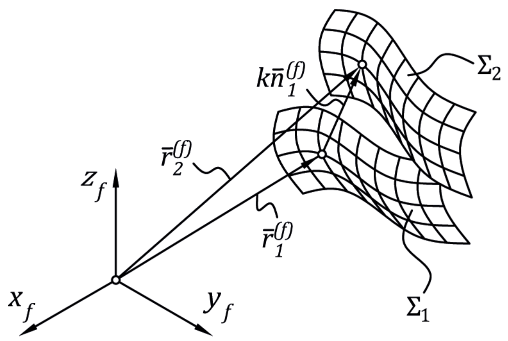

Figure 5. Determining distances between mating tooth surfaces

the solution should be approximated by means of a geometric method. The author proposes a method (Figure 6) wherein the gear tooth surface is presented as a grid of triangles, which can be accomplished by Delaunay triangulation [38].

Next, for each point on pinion tooth surface M_1, we shall determine point M_2, where the gear tooth surface triangle intersects with a straight line normal to the pinion tooth surface, which can be accomplished by the algorithm described in [39]. The points for which distance $|M_1M_2|$ is lower than the set distance are plotted on the chart, forming the gear pair's contact pattern.

RESULTS AND DISCUSSION

The proposed computation methods were visualised based on cylindrical gear pairs with data listed in Table 1.

Parameters of individual profiles together with their transverse sections were shown in Table 2.

The simulations enabled us to obtain *Ease-Off* charts, transmission charts, and contact patters for

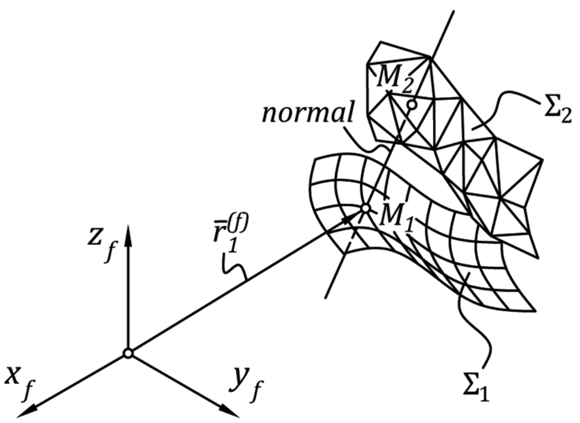

Figure 6. The proposed method for determining distances between mating tooth surfaces

the involute gear pair (Figure 7), Novikov gear pair (Figure 8), as well as eccentric-cycloidal (Figure 9) gear pair. In all cases, the modification which involves tooth flank line and profile crowning allowed us to avoid interference, as displayed by the consistent distribution of *Ease-Off* topography with minimum values present in the expected tooth contact areas. Moreover, transmission error did not occur, and the shape of the transmission curve was parabolic. In all cases, contact patters were determined for gear marking compound thickness $k=5\mu m$. Their areas as a function of pinion rotation angle were juxtaposed in Figure 10.

Used modification for involute gears results in a parabolic-like transmission chart (Figure 7b)), which is desirable and consistent with results obtained by other researchers [40,41]. Contact patterns are elliptical (Figure 7 c)) and also correspond to localized bearing contact for involute helical gearing [42]. In the case of the Novikov type of gearing, the transmission chart is flattened (Figure 8b)) with parabolic segments at the beginning and at the end of meshing. This shape of the transmission chart results from applied lead modification, which must be chosen not to reduce the overlap ratio (maintaining the constant transmission). Due to conformal contact *Ease-Off* plot (Figure 8a)) takes lower values than in the case of involute gearing (Figure 7a)). Contact patterns in Novikov gear are not elliptical and take the shape which is typical for high conformal gear pairs as reported in [20]. The transmission chart obtained for eccentric cycloidal gear mesh (Figure 9b)) is similar to that obtained for involute gearing (Figure 7b)). This similarity results from the fact that both of these gears are characterized by transverse and overlap ratios. Contact patterns are not elliptical (Figure 9c)). Its shape and location correspond to contact lines for this kind of gear mesh [21].

The largest contact area was found for the Novikov gear pair ($A=8.5\ mm^2$), due to the convexo-concave tooth contact. In other gear pairs, maximum areas of contact were $A=6.57\ mm^2$ for

Table 1. Basic gear mesh data

Parameter	Pinion	Gear
Number of teeth z	17	35
Toothed ring width b, mm	30	
Normal module m_n, mm	3	
Tooth helix line direction	Right	Left
Centre distance a_r, mm	84	

Table 2. Gear mesh parameters

Mesh	Parameters	Tooth profile (trasnverse section)
Involute mesh	α_n=20° β =20° r_{b1}=25.3047 mm r_{b2}=52.0979 mm r_1=27.1365 mm r_2=55.8693 mm x_{t1}=x_{t2}=0.1617	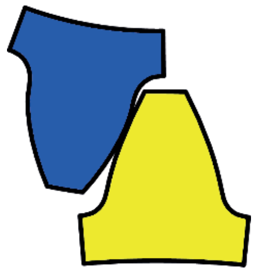
Novikov mesh	α_t=21.4036° β =21.7868° r_1=27.4615 mm r_2=56.5385 mm ρ_1=4.9431 mm ρ_2=4.9678 mm	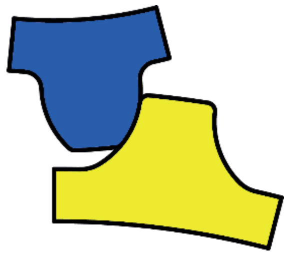
Eccentric-cycloidal mesh	β=21.7868° g=3.0208 mm v=-0.11 e=26.0885 mm r_1=27.4615 mm r_2=56.5385 mm	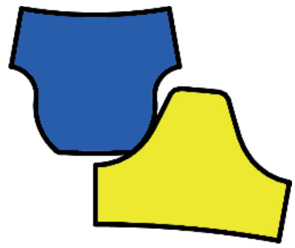

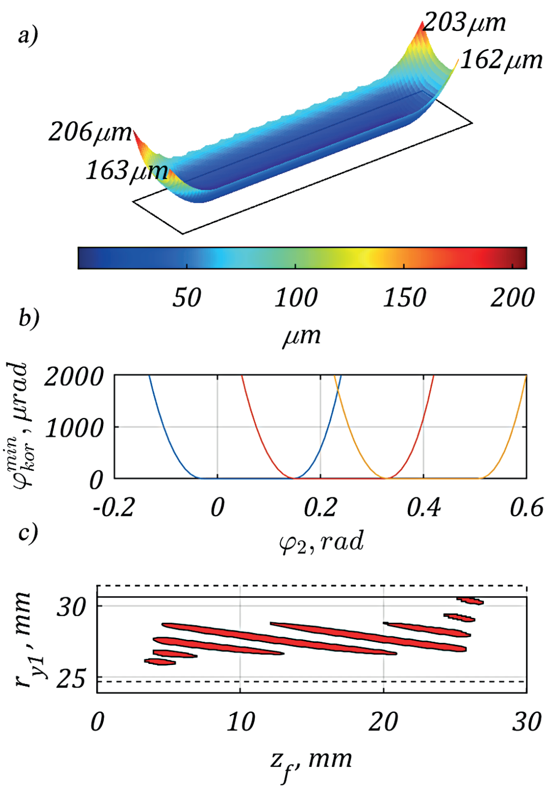

Figure 7. Results of tooth contact analysis for the involute gear pair: a) Ease-Off topography, b) transmission chart, c) contact patterns.

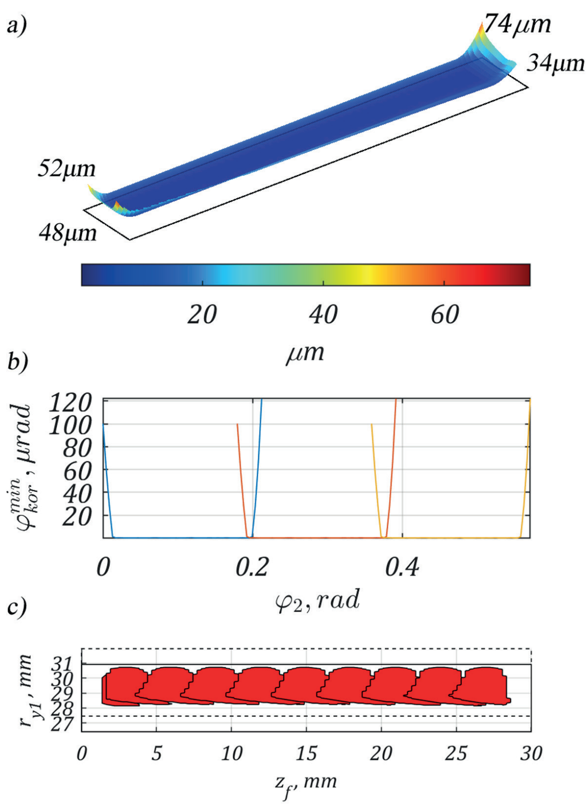

Figure 8. Results of tooth contact analysis for the Novikov gear pair: a) Ease-Off topography, b) transmission chart, c) contact patterns

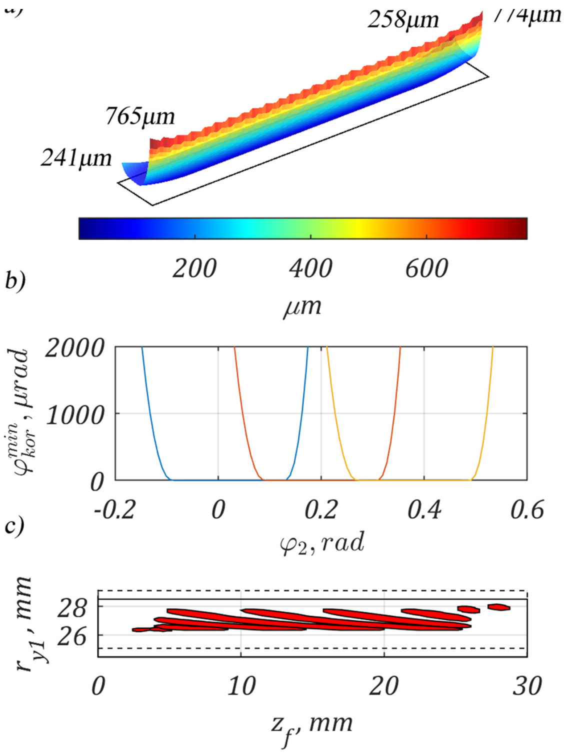

Figure 9. Results of tooth contact analysis for the eccentric-cycloidal gear pair: a) Ease-Off topography, b) transmission chart, c) contact patterns

involute and $A=5.32\ mm^2$ for eccentric-cycloidal gear. In addition, a reduced contact ratio in the Novikov gear relative to the other two gear pairs can be observed, caused by the character of tooth contact in the pair. Linear contact in the involute gear and the eccentric-cycloidal gear pair implies the presence of both face and overlap contact ratio, while in the Novikov type (with point contact), meshing takes place only as a result of the overlap.

CONCLUSIONS

The simulations allowed us to draw the following conclusions. Tooth modification involving crowning the addendum and the flank line enables avoiding edge contact. A suitably chosen modification ensures consistent transmission (no transmission error). The Novikov gear pair was characterised by the largest contact area (approx. 30% greater than for the involute gear pair, and 60% greater than for the eccentric-cycloidal gear pair).

Furthermore, assuming that the pinion's rotation speed is $n_1=100\ rpm$, the maximum sliding velocities are as follows: *102 mm/s* for the involute gear pair, *77 mm/s* for the Novikov gear pair and *99 mm/s* for the eccentric-cycloidal gear pair. The sliding velocity is lower nearly about 30% for Novikov gears. As it is known sliding velocity has a direct impact on the contact temperature which in turn is related to the wear of teeth.

Taking the above into account and assuming, for the sake of simplicity, that maximum contact stress is inversely proportional to the area of the contact ellipsis, the Novikov gear enables us to obtain a nearly 1.30-fold stress reduction. Therefore, we may posit a thesis that the Novikov gear pair will offer a greater surface load-carrying capacity (or durability arising from this capacity) than other types of meshing analysed in this paper, which may be tested in further research, both in the FEA environment and on test benches.

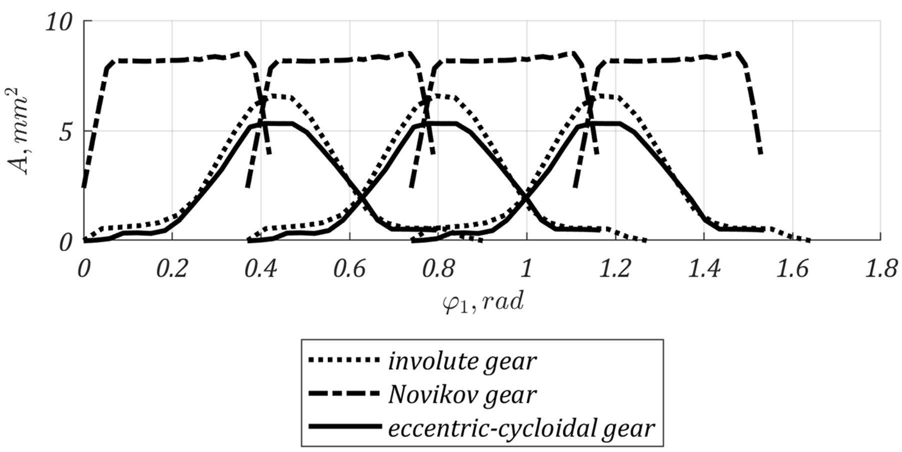

Figure 10. Contact areas as a function of pinion rotation angle.

REFERENCES

1. Pisula J., Budzik G., Przeszłowski Ł. An Analysis of the Surface Geometric Structure and Geometric Accuracy of Cylindrical Gear Teeth Manufactured with the Direct Metal Laser Sintering (DMLS) Method. Strojniski Vestnik/Journal of Mechanical Engineering. 2019; 65(2).
2. Budzisz W., Marciniec A. The New Gear Finishing Method Research for Highly Loaded Gears. Aerospace. 2022; 9(3).
3. Dziubek T., Sobolewski B., Budzik G., Gontarz M. Static Analysis of Selected Design Solutions for Weight-Reduced Gears. Advances in Science and Technology Research Journal. 2022; 16(3): 258–268.
4. Czerniec M., Świć A. Study of Contact Strength, Tooth Wear and Metal-Polymer Life of Worm Gears. Advances in Science and Technology Research Journal. 2022; 16(3): 143–154.
5. Okorn I., Nagode M., Klemenc J. Operating Performance of External Non-Involute Spur and Helical Gears: A Review. Strojniski Vestnik-Journal of Mechanical Engineering. 2021; 67(5): 256–271.
6. Li T., Xu H., Tian M. A Loaded Analysis Method for RV Cycloidal-pin Transmission Based on the Minimum Energy Principle. Strojniski Vestnik-Journal of Mechanical Engineering. 2020; 66(11): 655–667.
7. Batsch M., Markowski T., Legutko S., Krolczyk G.M. Measurement and mathematical model of convexo-concave Novikov gear mesh. Measurement. 2018; 125: 516–26.
8. Yang S.C. Mathematical model of a stepped triple circular-arc gear. Mechanism and Machine Theory. 2009; 44(5): 1019–1031.
9. Luo S., Wu Y., Wang J. The generation principle and mathematical models of a novel cosine gear drive. Mechanism and Machine Theory. 2008; 43(12): 1543–1556.
10. Liang D., Chen B., Tan R., Liao R. Geometric design and analysis of gear transmission with double circular arc-involute tooth profile. Proceedings of the Institution of Mechanical Engineers, Part C: Journal of Mechanical Engineering Science. 2017; 231(11): 2100–2109.
11. Hlebanja G., Hlebanja J., Okorn I. Research of Gears With Progressive Path of Contact. In: Proc. of 8th International Power Transmission and Gearing Conference, 2000, 215–221.
12. Chen Z., Ding H., Li B., Luo L., Zhang L., Yang J. Geometry and parameter design of novel circular arc helical gears for parallel-axis transmission. Advances in Mechanical Engineering. 2017; 9(2).
13. Chen Z., Zeng M., Fuentes-Aznar A. Computerized design, simulation of meshing and stress analysis of pure rolling cylindrical helical gear drives with variable helix angle. Mechanism and Machine Theory. 2020; 153: 103962.
14. Chen Z., Zeng M., Fuentes-Aznar A. Geometric Design, Meshing Simulation, and Stress Analysis of Pure Rolling Rack and Pinion Mechanisms. Journal of Mechanical Design. 2019; 142(3).
15. Chen Z., Lei B., Zeng M., Li Y., Fuentes-Aznar A. Computerized design, simulation of meshing and stress analysis of pure rolling internal helical gear drives with combined tooth profiles. Mechanism and Machine Theory. 2022; 104959.
16. Hlebanja G., Hlebanja J. Contribution to the Development of Cylindrical Gears. In: Power Transmissions. Springer, 2013, 309–320.
17. Zorko D., Kulovec S., Tavčar J., Duhovnik J. Different teeth profile shapes of polymer gears and comparison of their performance. Journal of Advanced Mechanical Design, Systems, and Manufacturing. 2017; 11(6).
18. Hlebanja G., Hlebanja J. S-gears: From Metal to Polymer Solution. In: Advanced Gear Engineering. Springer. 2018; 255–269.
19. Dyson A., Evans H.P., Snidle W. Wildhaber-Novikov circular arc gears: Geometry and Kinematics. Proceedings of The Royal Society A Mathematical Physical and Engineering Sciences. 1986; 403(1825): 313–349.
20. Radzevich S.P. High-conformal Gearing: Kinematics and Geometry. CRC Press, 2016.
21. Li X., Li C., Chen B., Liang D. Design and investigation of a cycloid helical gear drive. Journal of Mechanical Science and Technology. 2017; 31(9): 4329–4336.
22. Batsch M. Rapid Prototyping and Tooth Contact Analysis of Eccentric Cycloid Gear Mesh. Journal of KONBiN. 2019; 49(1): 369–382.
23. Batsch M. A novel method of obtaining honing tool profile for machining gears with profile modifications. ASME Journal of Manufacturing Science and Engineering. 2020; 142(9): 091004.
24. ISO 21771: 2007(E). Gears – Cylindrical involute gears and gear pairs – Concepts and geometry.
25. Klingelnberg J. Bevel Gear: Fundamentals and Applications. Springer, 2016.
26. Litvin F.L., Chen N.X., Chen J.S. Computerized determination of curvature relations and contact ellipse for conjugate surfaces. Computer Methods in Applied Mechanics and Engineering. 1995; 125(1): 151–170.
27. Pisula J. An analysis of the effect of the application of helical motion and assembly errors on the meshing of a spiral bevel gear using duplex helical method. Advances in Manufacturing Science and Technology. 2016; 40(1): 19–31.

28. Kawalec A., Wiktor J. Simulation of generation and tooth contact analysis of helical gears with crowned flanks. Proceedings of the Institution of Mechanical Engineers, Part B: Journal of Engineering Manufacture. 2008; 222(9): 1147–1160.
29. Sobolak M. Discrete numerical method of tooth contact analysis (TCA) with α-bufor use. Archives of Mechanical Technology and Automation. 2007; 27(2): 153–160.
30. Marciniec A., Pacana J., Pisula J., Fudali P. Comparative analysis of numerical methods for the determination of contact pattern of spiral bevel gears. Aircraft Engineering and Aerospace Technology. 2018; 90(2): 359–367.
31. Sobolak M. Analysis and synthesis of mating gear tooth surface by discrete methods. (Analiza i synteza współpracy powierzchni kół zębatych metodami dyskretnymi) Rzeszow University of Technol. Publ., 2006.
32. Johnson K.L. Contact mechanics. Cambridge University Press, 1987.
33. Batsch M., Homik W., Markowski T. Cylindrical Gears with Increased Contact Area – Proposal of Application in Watercrafts Power Transmission Systems. Solid State Phenomena. 2015; 236: 26–30.
34. Markowski T., Batsch M. Analytical and numerical methods to obtain contact pattern of convexo-concave Novikov gearing. Scientific Journal of Silesian University of Technology. Series Transport. 2014; (82): 155-165.
35. Batsch M., Markowski T. Influence of Novikov convexo-concave gear parameters on contact pattern. Scientific Journal of Silesian University of Technology Series Transport. 2015; 89: 89–99.
36. Levenberg K. A method for the Solution of Certain Problems in Least Squares. Quarterly of Applied Mathematics. 1944; 2(2): 164–168.
37. Marquardt D.W. An algorithm for least-squares estimation of nonlinear parameters. Journal of the society for Industrial and Applied Mathematics. 1963; 11(2): 431–441.
38. de Berg M., Cheong O., van Kreveld M., Overmars M. Computational Geometry: Algorithms and Applications. Springer, 2008.
39. Möller T., Trumbore B. Fast, Minimum Storage Ray-Triangle Intersection. Journal of Graphics Tools. 1997; 2(1): 21–28.
40. Litvin F.L, Fuentes A., Gonzalez-Perez I., Carvenali L., Kawasaki K., Handschuh R.F. Modified involute helical gears: computerized design, simulation of meshing and stress analysis. Computer Methods in Applied Mechanics and Engineering. 2003; 192(33): 3619–3655.
41. Litvin F.L., Fan Q., Vecchiato D., Demenego A., Handschuh R.F., Sep T.M. Computerized generation and simulation of meshing of modified spur and helical gears manufactured by shaving. Computer Methods in Applied Mechanics and Engineering. 2001; 190(39): 5037–5055.
42. Fuentes-Aznar A., Ruiz-Orzaez R., Gonzalez-Perez I. Comparison of spur, helical and curvilinear gear drives by means of stress and tooth contact analyses. Meccanica 2017; 52(7): 1721–1738.